

## Dynamics of pCO<sub>2</sub> and related air-ice CO<sub>2</sub> fluxes in the Arctic coastal zone (Amundsen Gulf, Beaufort Sea)

N.-X. Geilfus,<sup>1,2,3</sup> G. Carnat,<sup>4</sup> T. Papakyriakou,<sup>4</sup> J.-L. Tison,<sup>2</sup> B. Else,<sup>4</sup> H. Thomas,<sup>5</sup> E. Shadwick,<sup>5,6</sup> and B. Delille<sup>1</sup>

Received 11 March 2011; revised 27 October 2011; accepted 22 November 2011; published 2 February 2012.

[1] We present an Arctic seasonal survey of carbon dioxide partial pressure (pCO<sub>2</sub>) dynamics within sea ice brine and related air-ice CO<sub>2</sub> fluxes. The survey was carried out from early spring to the beginning of summer in the Arctic coastal waters of the Amundsen Gulf. High concentrations of pCO<sub>2</sub> (up to 1834 μatm) were observed in the sea ice in early April as a consequence of concentration of solutes in brines, CaCO<sub>3</sub> precipitation and microbial respiration. CaCO<sub>3</sub> precipitation was detected through anomalies in total alkalinity (TA) and dissolved inorganic carbon (DIC). This precipitation seems to have occurred in highly saline brine in the upper part of the ice cover and in bulk ice. As summer draws near, the ice temperature increases and brine pCO<sub>2</sub> shifts from a large supersaturation (1834 μatm) to a marked undersaturation (down to almost 0 μatm). This decrease was ascribed to brine dilution by ice meltwater, dissolution of CaCO<sub>3</sub> and photosynthesis during the sympagic algal bloom. The magnitude of the CO<sub>2</sub> fluxes was controlled by ice temperature (through its control on brine volume and brine channels connectivity) and the concentration gradient between brine and the atmosphere. However, the state of the ice-interface clearly affects air-ice CO<sub>2</sub> fluxes.

**Citation:** Geilfus, N.-X., G. Carnat, T. Papakyriakou, J.-L. Tison, B. Else, H. Thomas, E. Shadwick, and B. Delille (2012), Dynamics of pCO<sub>2</sub> and related air-ice CO<sub>2</sub> fluxes in the Arctic coastal zone (Amundsen Gulf, Beaufort Sea), *J. Geophys. Res.*, 117, C00G10, doi:10.1029/2011JC007118.

### 1. Introduction

[2] For both hemispheres, sea ice cover ranges between 18 and 28 million km<sup>2</sup> at its maximal extension [Comiso, 2003], and the sea ice zone is one of the largest biomes on Earth [Intergovernmental Panel on Climate Change, 2007]. It has been shown that sea ice has a strong impact on the global climate system through its control on albedo, air-sea exchange of heat, moisture and momentum, production of deep-water, stratification of surface waters during the spring melt and the seeding of primary production into the marginal ice zone [Dieckmann and Hellmer, 2010; Arrigo and Thomas, 2004].

[3] Each year, 7 Pg of anthropogenic carbon (C) are released to the atmosphere. Of this carbon release, 29% is

taken up by the oceans through physical and biological processes [Sabine et al., 2004]. According to the pCO<sub>2</sub> climatology of Takahashi et al. [2009], high latitude areas act as sinks for atmospheric CO<sub>2</sub>. It represents a direct pathway for CO<sub>2</sub> exchanges between the atmosphere and the ocean by mechanisms that are not yet fully understood [Rysgaard et al., 2007; Takahashi et al., 2002]. The lack of data in the polar areas, particularly with respect to sea-ice and gas exchange is therefore an important issue in the context of the oceanic uptake of atmospheric CO<sub>2</sub>. As pointed out by Tison et al. [2002], it is often assumed that sea ice prevents the atmosphere from exchanging CO<sub>2</sub> with the oceans. Moreover, in the pCO<sub>2</sub> climatology of Takahashi et al. [2009], the fluxes over sea ice covered areas are approximated by using pCO<sub>2</sub> data from underneath the ice. However, recent observations challenge this approach and suggest that sea ice could actually be a permeable medium allowing CO<sub>2</sub> exchanges with the atmosphere, during polar spring-summer [Papakyriakou and Miller, 2011; Semiletov et al., 2007; Delille, 2006; Zemmeling et al., 2006; Semiletov et al., 2004] but also during the winter [Miller et al., 2011; Heinesch et al., 2009]. Semiletov et al. [2004] suggested that melt ponds and open brine channels within sea ice represent a sink for atmospheric CO<sub>2</sub>, up to  $-39.3 \text{ mmol m}^{-2} \text{ d}^{-1}$ , during Arctic sea ice melt in June. Delille [2006] measured CO<sub>2</sub> fluxes, ranging from an uptake of  $-4 \text{ mmol m}^{-2} \text{ d}^{-1}$  to an evasion of  $+2 \text{ mmol m}^{-2} \text{ d}^{-1}$ , on Antarctic pack ice using chambers and linked these fluxes with the brine pCO<sub>2</sub>. This

<sup>1</sup>Unité d'Océanographie Chimique, Université de Liège, Liege, Belgium.

<sup>2</sup>Laboratoire de Glaciologie, DSTE, Université Libre de Bruxelles, Brussels, Belgium.

<sup>3</sup>Now at Center for Earth Observation Science, University of Manitoba, Winnipeg, Manitoba, Canada.

<sup>4</sup>Center for Earth Observation Science, University of Manitoba, Winnipeg, Manitoba, Canada.

<sup>5</sup>Department of Oceanography, University of Dalhousie, Halifax, Nova Scotia, Canada.

<sup>6</sup>Now at Center for Marine and Atmosphere Research, Commonwealth Scientific and Industrial Research Organisation, Hobart, Tasmania, Australia.

link was also identified by *Nomura et al.* [2010a], who measured CO<sub>2</sub> fluxes ranging from  $-1 \text{ mmol m}^{-2} \text{ d}^{-1}$  to  $+0.7 \text{ mmol m}^{-2} \text{ d}^{-1}$  in first year landfast sea ice in late May 2008 in Barrow, Alaska. During winter, brine pCO<sub>2</sub> becomes supersaturated with respect to the atmosphere as sea ice temperature decreases, and brine salinity increases [Papadimitriou et al., 2004]. CO<sub>2</sub> can then be emitted from brine channels to the underlying water and, if the ice is permeable, to the overlying atmosphere [Loose et al., 2011; Rysgaard et al., 2007; Nomura et al., 2006; Papadimitriou et al., 2004].

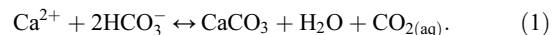
[4] During sea ice growth, most of the impurities (solutes, gases and particular matter) cannot be incorporated into the ice matrix and are rejected at the advancing ice-water interface. This brine rejection influences the release of dissolved gases and solutes into the water column [Papadimitriou et al., 2004]. However, some of the impurities are retained in liquid inclusions or as gas bubbles within the solid ice matrix. This has important consequences for the microstructure and properties of sea ice, both of which being heavily influenced by the relative brine volume [Eicken, 2003]. Sub-ice pCO<sub>2</sub> has been shown to be greater than atmospheric values in both the Arctic Ocean [Semiletov et al., 2007, 2004] and the Southern Ocean [Delille, 2006; Gibson and Trull, 1999]. High dissolved inorganic carbon (DIC) concentrations have also been reported below Arctic sea ice [Anderson et al., 2004]. Low total alkalinity (TA) and DIC concentrations, relative to surface waters, have been described in sea ice brine in the Antarctic during the summer, while high TA and DIC concentrations have been reported during the winter [Papadimitriou et al., 2007; Delille, 2006; Gleitz et al., 1995].

[5] In addition, sea ice affects pCO<sub>2</sub> of the underlying water column and then the budget of air-sea CO<sub>2</sub> fluxes of Arctic Ocean open waters [Shadwick et al., 2011; Bates and Mathis, 2009; Fransson et al., 2009]. Air-sea CO<sub>2</sub> fluxes are likely to change in the context of global warming [Cai et al., 2010], one of the main forcing being sea ice retreat. Collectively these observations indicate that sea ice likely effects the vertical transport of CO<sub>2</sub> in the polar marine environments. It follows that in order to predict future change of air-sea CO<sub>2</sub> fluxes in Arctic Ocean, the role of sea ice in the overall budget of air-sea CO<sub>2</sub> must be understood.

[6] The chemical composition of sea ice is primarily a function of salinity and temperature, but is further modified by productivity of the internal microbial assemblages recruited from the surface water during sea ice formation [Dieckmann and Hellmer, 2010]. Because of the strong influence of biological activity on the composition of natural sea ice brine, little attention has been paid to the potential contribution of abiotic processes, such as gas exchanges or mineral formation [Papadimitriou et al., 2007]. The increase of salinity at low temperature in the ice induces changes in the mineral-liquid and gas-liquid thermodynamic equilibrium that could lead to a degassing and/or a mineral precipitation from the highly concentrated brine [Munro et al., 2010; Papadimitriou et al., 2007, 2004; Marion, 2001; Killawee et al., 1998]. Rysgaard et al. [2007] suggested that precipitation of carbonate minerals within sea ice during winter growth, and associated release of CO<sub>2</sub> to the underlying ocean with brine rejection, could drive a significant CO<sub>2</sub> uptake from the atmosphere on sea ice warming in the

spring. This precipitation was observed for the first time by *Dieckmann et al.* [2008, 2010] in Antarctic and Arctic sea ice, respectively. Calcium carbonate was found under the form of the mineral ikaite (CaCO<sub>3</sub> · 6H<sub>2</sub>O). According to both *Papadimitriou et al.* [2004] and *Rysgaard et al.* [2007], precipitation of CaCO<sub>3</sub> can occur during fall and winter within growing sea ice.

[7] Precipitation of calcium carbonate in standard seawater conditions is described by:



[8] As the temperature of sea ice decreases, so does the brine volumes in the ice. This leads to an increase in concentration of calcium (Ca<sup>2+</sup>) and bicarbonate (HCO<sub>3</sub><sup>-</sup>) ions, which may later combine to form CaCO<sub>3</sub>. This synthesis results in a release CO<sub>2(aq)</sub> (equation (1)).

[9] DIC is defined by the equation:

$$\text{DIC} = [\text{HCO}_3^-] + [\text{CO}_3^{2-}] + [\text{CO}_2]. \quad (2)$$

[10] Total alkalinity can be described by:

$$\text{TA} = [\text{HCO}_3^-] + 2[\text{CO}_3^{2-}] + [\text{B}(\text{OH})^-] + [\text{OH}^-] - [\text{H}^+]. \quad (3)$$

[11] The precipitation of one mole of CaCO<sub>3</sub> reduces DIC by one mole and TA by two moles, and drives the system to higher pCO<sub>2</sub> (Figure 1). Dissolution of CaCO<sub>3</sub> in standard seawater conditions corresponds to the reverse of equation (1).

[12] According to *Delille* [2006] and coworkers, precipitation of CaCO<sub>3</sub> can occur at different depths in the ice. Depending on the physical conditions at the location where the precipitation takes place, the impact on the net budget of CO<sub>2</sub> fluxes from the ice to the atmosphere will be very different, depending on the timing of this precipitation and sea ice permeability. Hence, CaCO<sub>3</sub> precipitation could promote CO<sub>2</sub> uptake from the atmosphere [Rysgaard et al., 2009, 2007], but release of CO<sub>2</sub> can be possible in some case [Delille, 2006].

[13] In this paper, we present results from the largest survey ever performed on the pCO<sub>2</sub> dynamics within sea ice, from early spring to the beginning of the Arctic summer. Ice cores and brine samples were analyzed for temperature, salinity, TA, DIC, chlorophyll-a (Chl a) concentrations as well as for dry-extraction measurements of pCO<sub>2</sub>. We investigate CO<sub>2</sub> fluxes at the sea ice interface with the atmosphere and correlate these with the pCO<sub>2</sub> dynamics observed in the brine channels.

## 2. Study Site, Materials, and Methods

[14] Data presented in this paper were collected on board the *CCGS Amundsen* during the International Polar Year – Circumpolar Flaw Lead system study (IPY-CFL 2008). This project was carried out in the Amundsen Gulf, Beaufort Sea, Canada, located on 70° 30' N, 120° 30' W. Samples were collected at individual stations between April and June 2008, from the beginning of spring until the beginning of summer

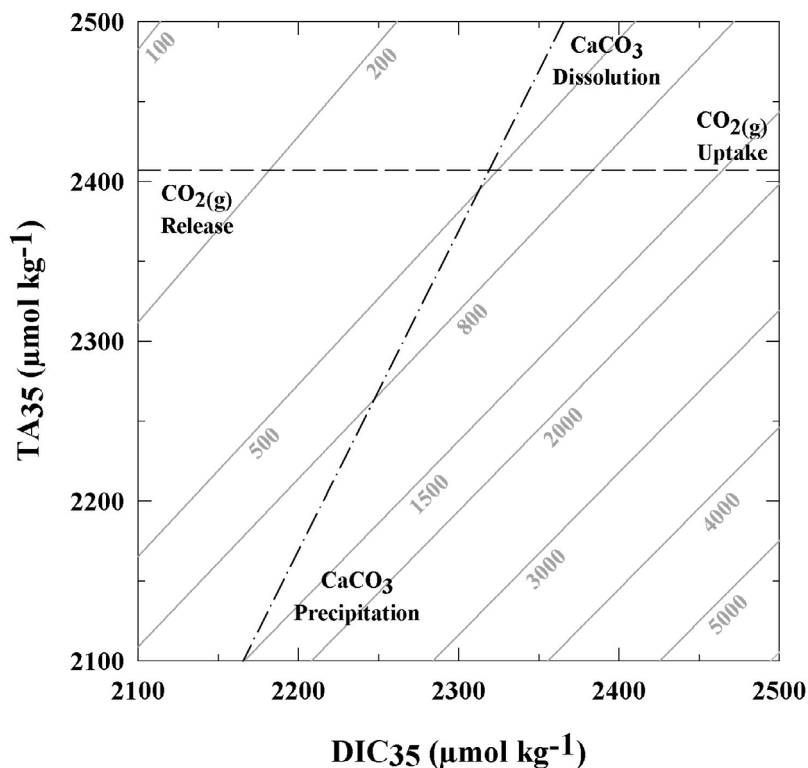


**Figure 1.** Theoretical effects of CaCO<sub>3</sub> precipitation – dissolution and CO<sub>2</sub> release – uptake on DIC and TA (dashed lines). Gray lines indicate levels of constant pCO<sub>2</sub> (in μatm).

(Figure 2, Table 1). It is therefore important to note that the results potentially integrate both spatial and temporal variability.

[15] Sampling was achieved within an area of about 25 m<sup>2</sup> in order to minimize bias from spatial heterogeneity. The sample area was always located upwind of the ship to avoid any contamination from activities on the research vessel. The first part of a sampling day was dedicated to ice core extraction after which the group collected brine from sack holes and undertook in situ measurements. Seawater was typically collected from the first ice core and was sampled at the ice-water interface.

[16] A Teflon coated stainless steel corer with an internal diameter of 7 cm was used to retrieve ice cores. Cores were immediately wrapped in polyethylene (PE) bags and stored on the sampling site in an insulated box filled with individual cooling bags, pre-cooled at –70°C. This precaution served to minimize brine drainage from samples [Tison *et al.*, 2008].

[17] A dedicated ice core for bulk ice measurements of TA and DIC was processed in the field. The top and bottom 15 cm, as well as the central part of the ice core, were cut off and placed immediately in a gas-tight laminated NEN/PE plastic bag fitted with a gas-tight Tygon tube and valve for sampling. A solution of supersaturated HgCl<sub>2</sub> was added to the plastic bag to halt biological activity. The bag was immediately closed, and excess air was removed through a tube using manual air pump. The ice was allowed to completely melt at +4°C in the dark, after which DIC and TA analysis were immediately undertaken. The maximum potential leakage has been estimated to less than 20 μmol

kg<sup>-1</sup> by Miller *et al.* [2011]. This error is consistent with our own assessment at high pCO<sub>2</sub> in the conditions encountered during the survey. Sackholes were drilled at different depths, ranging from about 15 cm. Brines, from adjacent brine channels and pockets, seeped into the sackholes for 10–60 min before being collected using a peristaltic pump (Cole Palmer, Masterflex - Environmental Sampler) [Gleitz *et al.*, 1995]. Each sackhole remained covered with a plastic lid to minimize mixing with the free-atmosphere. Under ice seawater was also collected using the same peristaltic pump at the ice-water interface and at 1 m depth.

[18] Sea ice temperature was measured in situ directly after extraction of the core using a calibrated probe (TESTO 720) inserted into pre-drilled holes (~3 cm depth) perpendicular to core sides. The hole diameter matched that of the temperature probe. Precision of the measurements was ±0.1°C. Bulk ice salinity was determined on board from melted ice sections at +4°C with a calibrated Thermo-Orion portable salinometer WP-84TPS meter with a precision of ±0.1. Ice sections were cut from successive 5 cm thick slices of a dedicated ice core. These sections were then melted in the dark at +4°C to perform Chl *a* measurements that were carried out using the extraction method described by Parsons *et al.* [1984].

[19] DIC and TA were measured on melted bulk ice, brine and seawater samples. Brine and seawater samples were poisoned with a solution of supersaturated HgCl<sub>2</sub> and samples were stored in the dark, at +4°C until analysis. The concentration of DIC and TA in melted bulk ice, brine and seawater were all analyzed on board by coulometric and potentiometric titration, respectively, using a VINDTA 3C

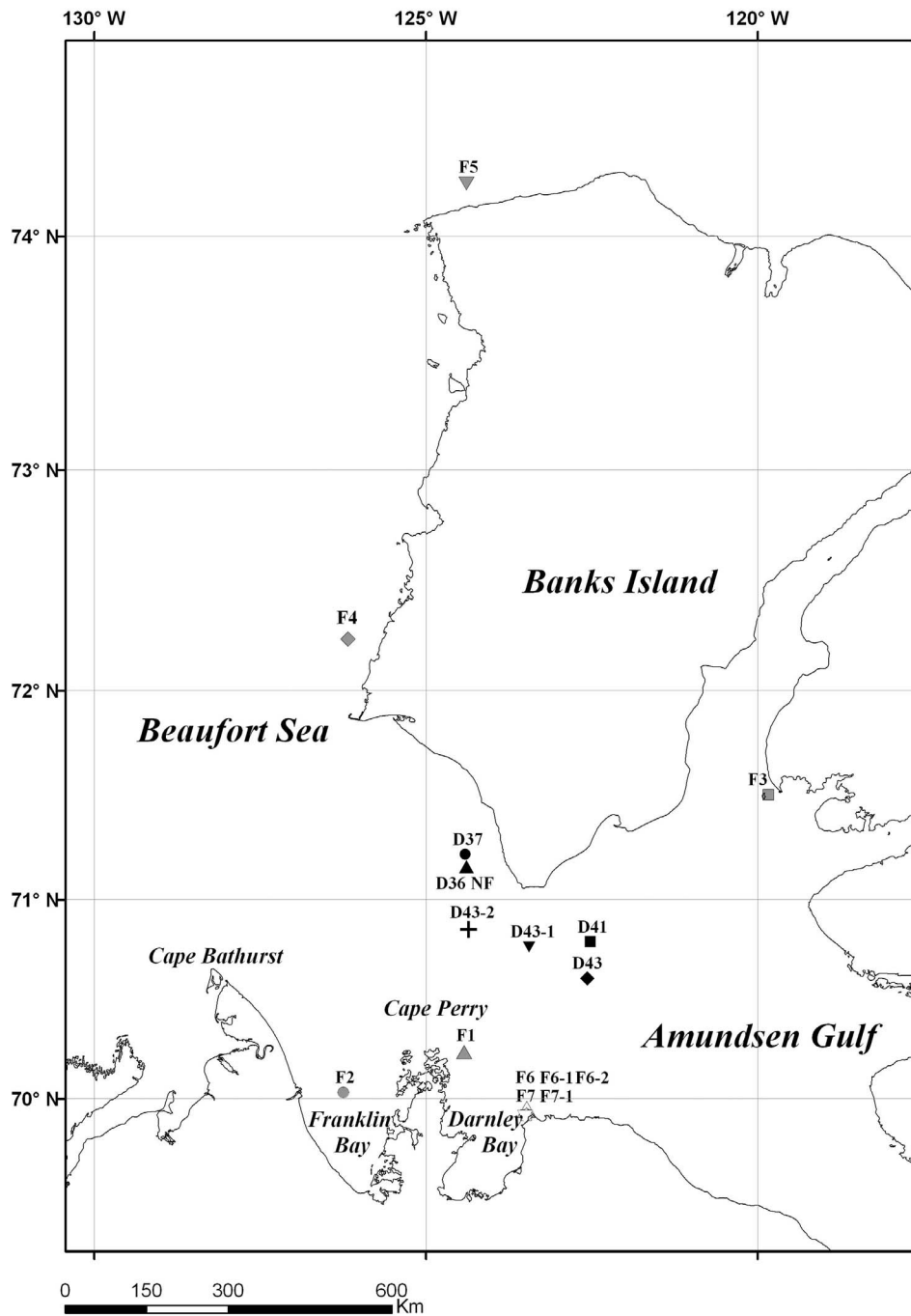


**Figure 2.** Map of the CFL study area in the Amundsen Gulf (NT, Canada) indicating the locations of the sampling stations where the CO<sub>2</sub> data was collected.

(Versatile Instrument for the Determination of Titration Alkalinity, by Marianda). The description of this procedure is detailed by *Shadwick et al.* [2011], according to *Johnson et al.* [1993] and *Dickson et al.* [2007]. Routine analyses of Certified Reference Materials (provided by A. G. Dickson, Scripps Institution of Oceanography) ensured that the uncertainty of the DIC and TA measurements were less than  $2 \mu\text{mol kg}^{-1}$  and  $3 \mu\text{mol kg}^{-1}$ , respectively.

[20] The pCO<sub>2</sub> of brine and seawater from underneath the ice was measured in situ using a custom made equilibration

system [*Delille et al.*, 2007]. The system consisted of a membrane contractor equilibrator (Membrana, Liqui-cell) that was connected to a non-dispersive infrared gas analyzer (IRGA, Li-Cor 6262) via a closed air loop. Brine and airflow rates through respectively the equilibrator and IRGA were approximately  $2 \text{ L min}^{-1}$  and  $3 \text{ L min}^{-1}$ . Temperature was simultaneously measured in situ and at the outlet of the equilibrator using Li-Cor temperature sensors. Temperature correction of pCO<sub>2</sub> was applied assuming that the relation of *Copin-Montégut* [1988] is valid at low temperature and high

**Table 1.** Dates of the Sampling Stations<sup>a</sup>

Station	Date
D36	April 6
D37	April 11
D41	April 16
D43	April 26
D43–1	April 29
D43–2 <sup>b</sup>	May 2
F1	May 9
F2	May 13
F3	May 20
F4	May 24
F5	May 28
F6	June 2
F6–1	June 7
F6–2	June 9
F7	June 12
F7–1	June 18

<sup>a</sup>The “D” stations were sampled on drifting sea ice (pack ice) while the “F” stations were sampled on landfast sea ice.

<sup>b</sup>Station D43–2 was sampled in May but as it was on same location as station D43 and D43–1, we decided to regroup them in April.

salinity. The IRGA was calibrated soon after returning on the ship while the analyzer was still cold. Data were stored on a Li-Cor Li-1400 data logger. All the devices, except the peristaltic pump, were enclosed in an insulated box that contained a 12 V power source providing enough warming to keep the inside temperature just above 0°C.

[21] The CO<sub>2</sub> fluxes at the upper sea ice surface were measured using an accumulation (West system). The chamber is a metal cylinder closed at the top, with an internal diameter of 20 cm and an internal height of 9.7 cm. A rubber seal surrounded by a serrated – edge steel ensures an air – tight connection between the ice and the chamber of accumulation. For measurement over snow, a steel tube was mounted at the base of the chamber to enclose snow down to the ice and prevent lateral infiltration of air through the snow. The chamber was connected in a closed loop to the IRGA with an air pump rate at 3 L min<sup>-1</sup>. The measurement of pCO<sub>2</sub> in the chamber was recorded every 30 s for at least 5 min. The flux was computed from the slope of the linear regression of pCO<sub>2</sub> against time ( $r^2 > 0.99$ ) according to *Frankignoulle* [1988], taking into account the volume of ice or snow enclosed within the chamber. The uncertainty of the flux computation due to the standard error on the regression slope was on average  $\pm 3\%$ .

### 3. Results

#### 3.1. Background Measurements

[22] Drift sea ice was sampled in April (stations D36 to D43–2) while landfast sea ice was sampled from May to June (stations F1 to F7–1) (Figure 3). Our reference to Figure 3 is limited to the interpretation of the CO<sub>2</sub> data. A companion paper (G. Carnat et al., Year-round survey of Arctic sea ice physical properties during the CFL project, manuscript in preparation, 2012) describes in detail the thermodynamic evolution of the sea ice cover during the whole survey. In April, bulk ice salinity profiles (Figure 3b) presented a well-marked C-shape while the brine salinity exhibited a strong vertical gradient, driven by the temperature profile (Figure 3a). Apart from the warm bottom sea ice base, the ice

was mainly under the permeability threshold of 5% for columnar ice (Figure 3c). These stations were typical of a late winter situation. Bulk ice salinity at the surface decreased with a minimal value observed at the end of the month. The brine salinity decreased as well. The ice was beyond the permeability threshold. These stations were typical of a warming period. Finally, in June, the ice temperature profiles became isothermal, around  $-1^\circ\text{C}$ , with a maximal temperature observed at the top of the ice. Bulk ice as well as brine salinity were marked by a minimum at the top. The ice was highly permeable. These characteristics are typical of a decaying sea ice cover.

[23] The sea ice concentration of Chl a ranged from below 0.01  $\mu\text{g L}^{-1}$  up to 1330  $\mu\text{g L}^{-1}$  (Figure 3d). From April to May, Chl a concentration in bottom sea ice increased significantly from 130  $\mu\text{g L}^{-1}$  to 1330  $\mu\text{g L}^{-1}$  then decreased to 1  $\mu\text{g L}^{-1}$  in June. Our Chl a concentrations are consistent with values reported by *Mundy et al.* [2011] and *Song et al.* [2011] during this survey and by *Riedel et al.* [2008] in the same area in 2004.

[24] Brine temperature for the sampling stations ranged from  $-8.5^\circ\text{C}$  in April to  $0^\circ\text{C}$  in June (Figure 4a). By mid-May brine temperature approached that of the underlying seawater, and then stabilized around  $0^\circ\text{C}$  thereafter. Brine salinity decreased from 137.4 in April to 0 in June (Figure 4b) in response to the seasonally rise in temperature. Brine salinity actually dropped below seawater salinity in late May. Seawater salinity at the ice-water interface remained fairly constant (between 33.2 and 30.7) until late May and then decreased slightly to 26.4, with very low values of 2.9 and 6.9 observed at F6–1 and F7, respectively.

#### 3.2. Inorganic Carbon

[25] In April, it was not possible to collect brine samples at all depths due the small volume of brine available (Figure 3c). Brine pCO<sub>2</sub> were supersaturated (relative to atmospheric concentration) throughout the sea ice, ranging between 1839  $\mu\text{atm}$  to 465  $\mu\text{atm}$  (Figure 5). The maximum brine pCO<sub>2</sub> was observed in the middle of the ice column. Variation in pCO<sub>2</sub> with depth declined in May, with pCO<sub>2</sub> decreasing from F1 to F4. The brine pCO<sub>2</sub> remained supersaturated (between 389  $\mu\text{atm}$  to 888  $\mu\text{atm}$ ), except at the 2 bottom most brine sampling depths, where a pCO<sub>2</sub> of 147  $\mu\text{atm}$  and 306  $\mu\text{atm}$  was observed at F2 and F4 respectively. Brine pCO<sub>2</sub> declined significantly by June, at which time it was highly undersaturated with respect to the atmosphere, with values ranging from 188  $\mu\text{atm}$  to 0  $\mu\text{atm}$ . The pCO<sub>2</sub> in the melt ponds ranged between 79  $\mu\text{atm}$  to 348  $\mu\text{atm}$ .

[26] The pCO<sub>2</sub> of the underlying water ranged from 528  $\mu\text{atm}$  to 5  $\mu\text{atm}$  (Figure 4c) over the sampling period. In April, seawater pCO<sub>2</sub> was relatively stable near to atmospheric levels (396  $\mu\text{atm}$ ). In early May, seawater pCO<sub>2</sub> increased, reaching 528  $\mu\text{atm}$ , and then declined to a marked undersaturation by June, with some measurements approaching 5  $\mu\text{atm}$ . The low summer seawater pCO<sub>2</sub> is associated with a reduction in seawater salinity (Figure 4c). The pCO<sub>2</sub> of both underlying water and brine passed below the threshold of saturation at the same time. At some time, seasonal variation of pCO<sub>2</sub> of the underlying water does not mimic seasonal pattern presented by *Shadwick et al.* [2011]. However, the pCO<sub>2</sub> values of *Shadwick et al.* [2011] are underway pCO<sub>2</sub> data collected water at 3 m deep and averaged both spatially (over a

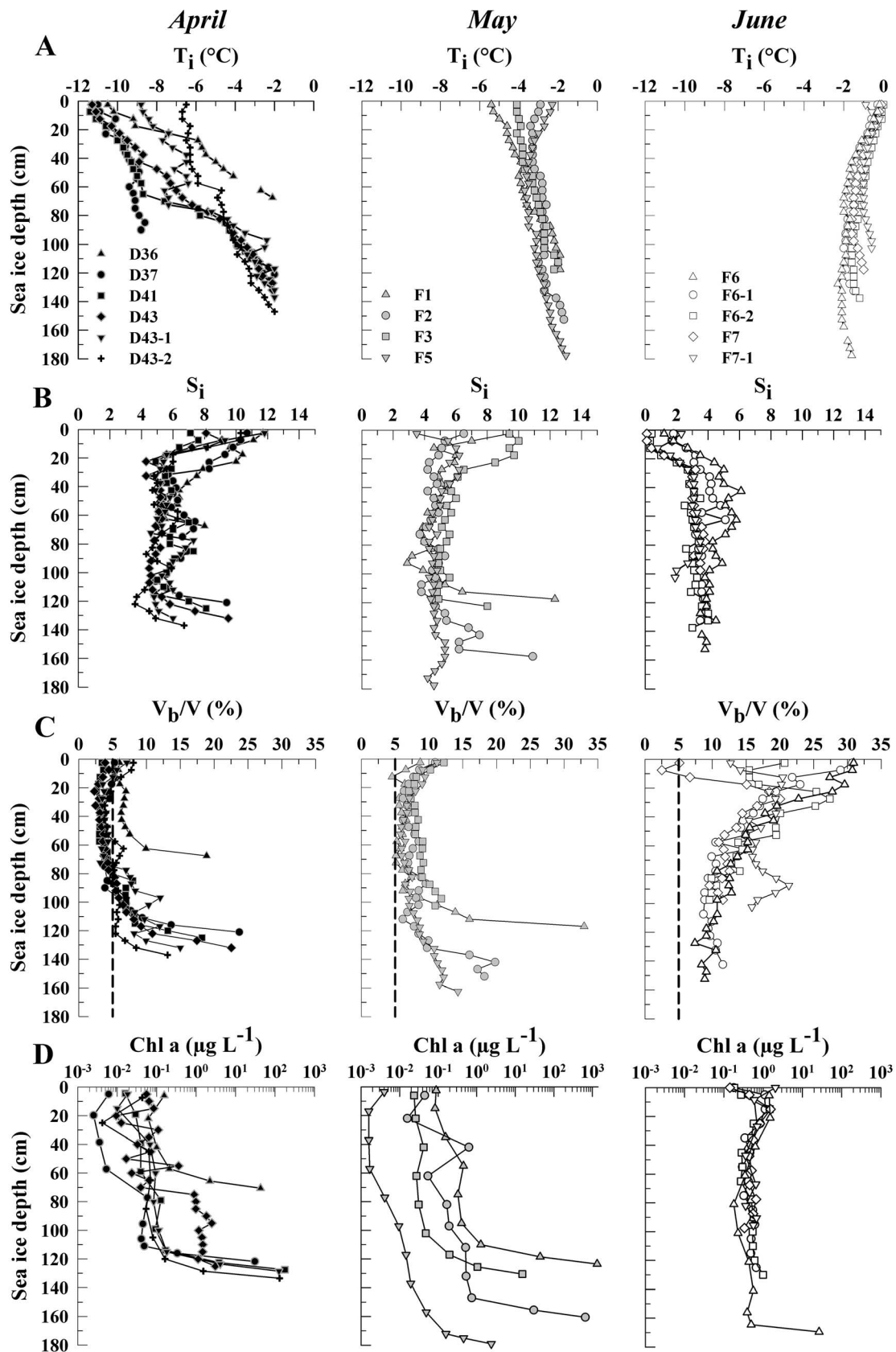


**Figure 3.** Sea ice conditions for the CFL stations considered, including (a) temperature profile,  $T_i$ , (b) salinity profile,  $S_i$ , (c) relative brine volume,  $V_b/V$ , and (d) Chl a concentration. NB: during June, the data at a depth of 0 represents the melt ponds.

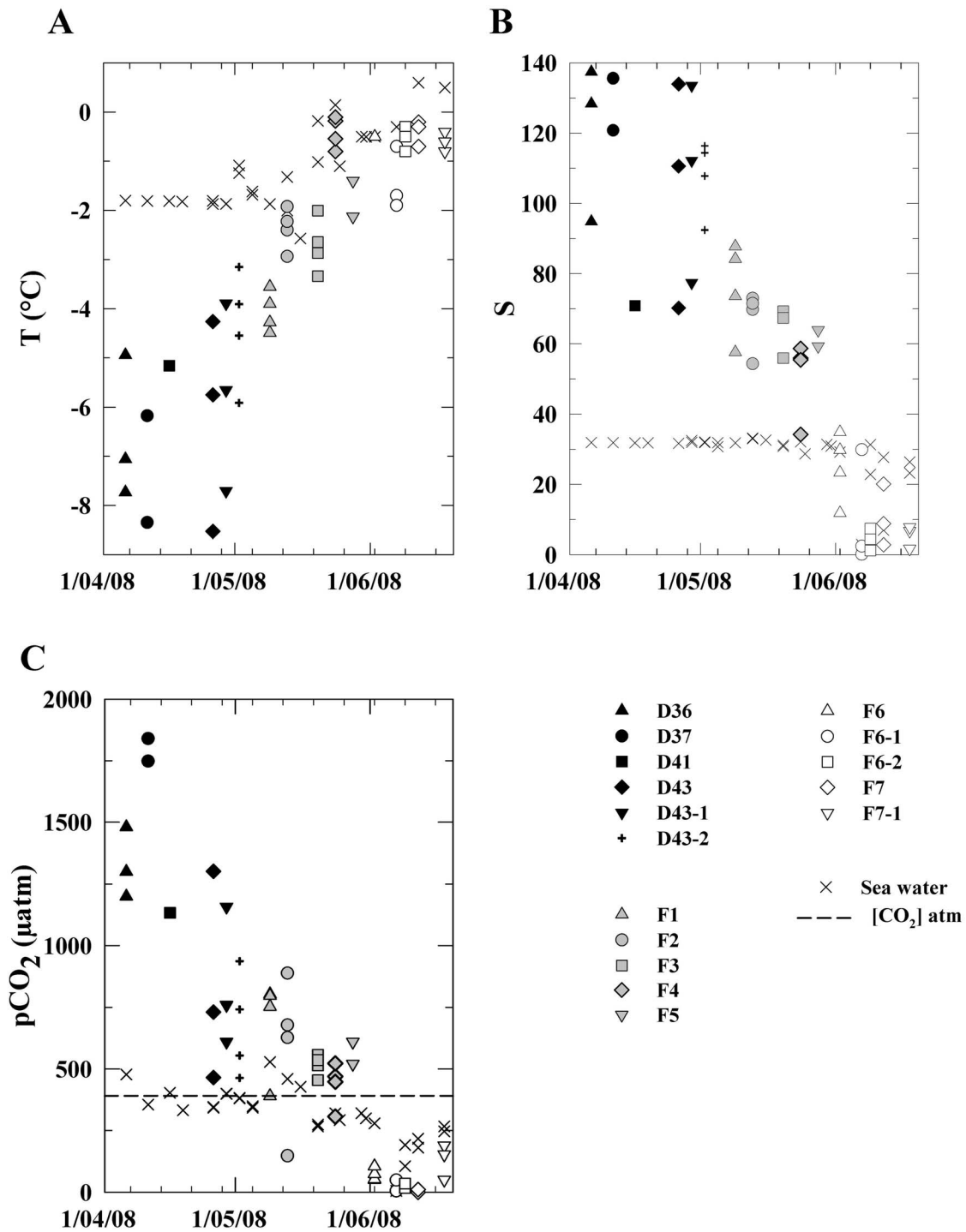


**Figure 4.** Temporal evolution of brine and seawater (a) temperature, (b) salinity, and (c) pCO<sub>2</sub> for the CFL stations considered.

larger region than that presented here) and temporally (monthly), while the data presented here was discrete measurement at the ice-water interface.

[27] TA and DIC in brine ranged from 173  $\mu\text{mol kg}^{-1}$  to 8191  $\mu\text{mol kg}^{-1}$  and from 165  $\mu\text{mol kg}^{-1}$  to 8254  $\mu\text{mol kg}^{-1}$ , respectively. TA and DIC in bulk sea ice ranged from 69  $\mu\text{mol kg}^{-1}$  to 635  $\mu\text{mol kg}^{-1}$  and 177  $\mu\text{mol kg}^{-1}$  to 613  $\mu\text{mol kg}^{-1}$ , respectively (Figures 6a and 6b). In

seawater samples, TA and DIC ranged from 331  $\mu\text{mol kg}^{-1}$  to 2280  $\mu\text{mol kg}^{-1}$  and 301  $\mu\text{mol kg}^{-1}$  to 2210  $\mu\text{mol kg}^{-1}$ , respectively. Both TA and DIC for bulk sea ice and seawater samples are of the same order of magnitude as those reported by *Miller et al.* [2011] and *Rysgaard et al.* [2007], who both presented TA and DIC measurement from landfast sea ice in Franklin Bay, Canada.

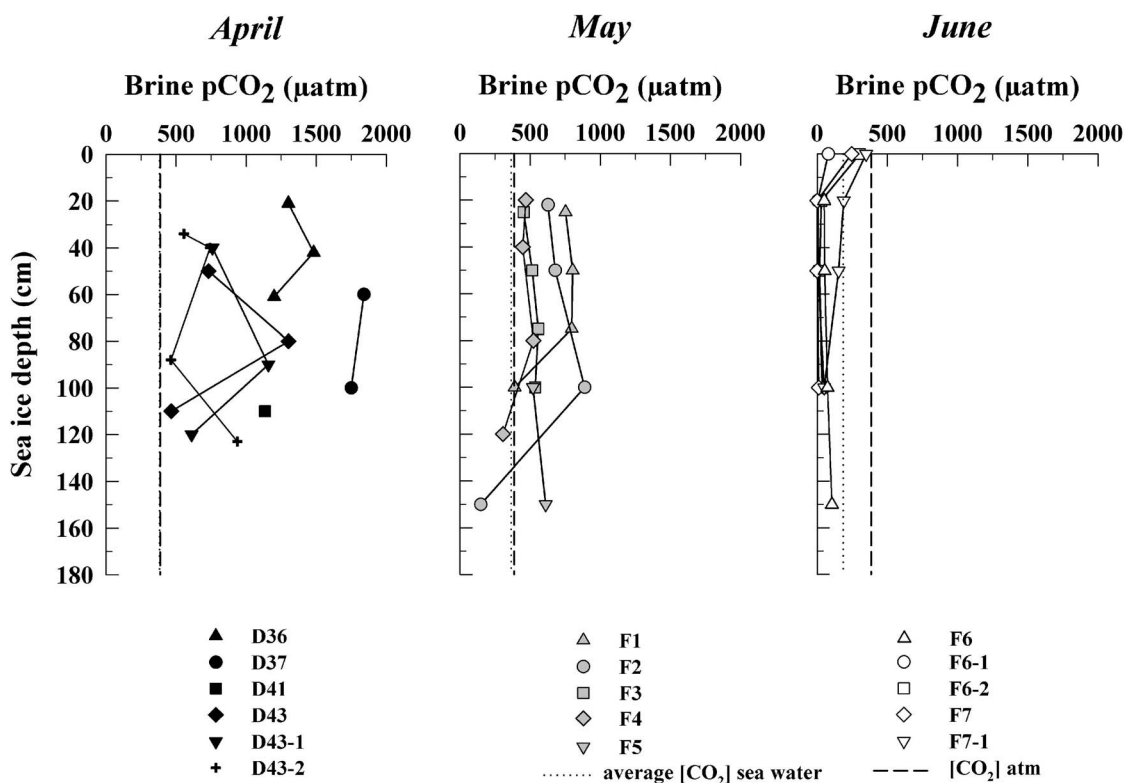


**Figure 5.** Profiles of direct in situ brine pCO<sub>2</sub> measurements for the three groups of stations considered. The seawater pCO<sub>2</sub> (dotted line) is an average for the considered month.

### 3.3. CO<sub>2</sub> Fluxes

[28] CO<sub>2</sub> fluxes were measured over sea ice, on sea ice, melt ponds, superimposed ice (Figure 7a) and on snow cover (Figure 7b). The CO<sub>2</sub> fluxes at the sea ice interface ranged from +0.84 mmol m<sup>-2</sup> d<sup>-1</sup> to -2.63 mmol m<sup>-2</sup> d<sup>-1</sup> (where a positive value indicates a CO<sub>2</sub> released from the ice surface to the atmosphere) while fluxes over snow cover ranged between +2.1 mmol m<sup>-2</sup> d<sup>-1</sup> and -1.49 mmol m<sup>-2</sup> d<sup>-1</sup>. No fluxes were detected on superimposed ice. Strong negative fluxes were measured over melt ponds, ranging from -0.13 mmol m<sup>-2</sup> d<sup>-1</sup> to -2.65 mmol m<sup>-2</sup> d<sup>-1</sup>. Observed fluxes over the sea ice were similar to measurements reported in Barrow (Alaska) or in the Hokkaido island (Japan) by *Nomura et al.* [2010a, 2010b], respectively, and by *Delille* [2006] and coworkers in Antarctica, using similar chamber techniques. Note that fluxes were also not detected on superimposed sea ice by *Nomura et al.* [2010b] and *Delille* [2006] and coworkers.

[29] No fluxes were detected for ice surface temperature below -10°C, with the exception of a small negative flux of -0.23 mmol m<sup>-2</sup> d<sup>-1</sup> to -0.6 mmol m<sup>-2</sup> d<sup>-1</sup> at stations D36 and D37, respectively. As the temperature of the ice increased from -10°C to -6°C, a positive flux was observed with a maximum value of +0.84 mmol m<sup>-2</sup> d<sup>-1</sup>. Finally, from -6°C to 0°C, negative fluxes with a maximum value of -2.6 mmol m<sup>-2</sup> d<sup>-1</sup> were observed. On snow, flux trends were much less clear with higher temporal variability. Fluxes ranged from -1.49 mmol m<sup>-2</sup> d<sup>-1</sup> to +2.1 mmol m<sup>-2</sup> d<sup>-1</sup>. The overall pattern is similar to fluxes over the ice,

but with a large number of observations showing negligible fluxes and a few outliers, with higher values than over the ice, both positive and negative, with no relationship to the air and ice temperature.

## 4. Discussion

[30] Inorganic carbon dynamics in the ocean is affected by several processes, including temperature and salinity changes, precipitation or dissolution of CaCO<sub>3</sub> and biological activity [*Zeebe and Wolf-Gladrow*, 2001]. This holds true for sea ice, yet changes in temperature and salinity are enhanced compared to the water column.

### 4.1. Effects of Primary Production

[31] Evaluating primary production within sea ice, and the related impact on brine pCO<sub>2</sub> has proven difficult [*Delille et al.*, 2007]. A common indicator of primary production is the change in autotrophic biomass. A rough measure of algal biomass is algal pigment concentration (Chl a). Chl a in sea ice varies by geographic region, ice type and seasons [*Arrigo et al.*, 2010].

[32] In April and May, while Chl a concentration values remained below 1.7 µg L<sup>-1</sup> in brine, a large increase of Chl a concentration up to 1330 µg L<sup>-1</sup> of bulk ice at the bottom was observed. Such build-up of Chl a suggests sustained primary production that potentially consumes CO<sub>2</sub>, i.e., reducing both sea ice DIC and brines pCO<sub>2</sub>. An enhanced pCO<sub>2</sub> decrease was observed at the time of the sympagic algal bloom in April and May and corresponded in time to a

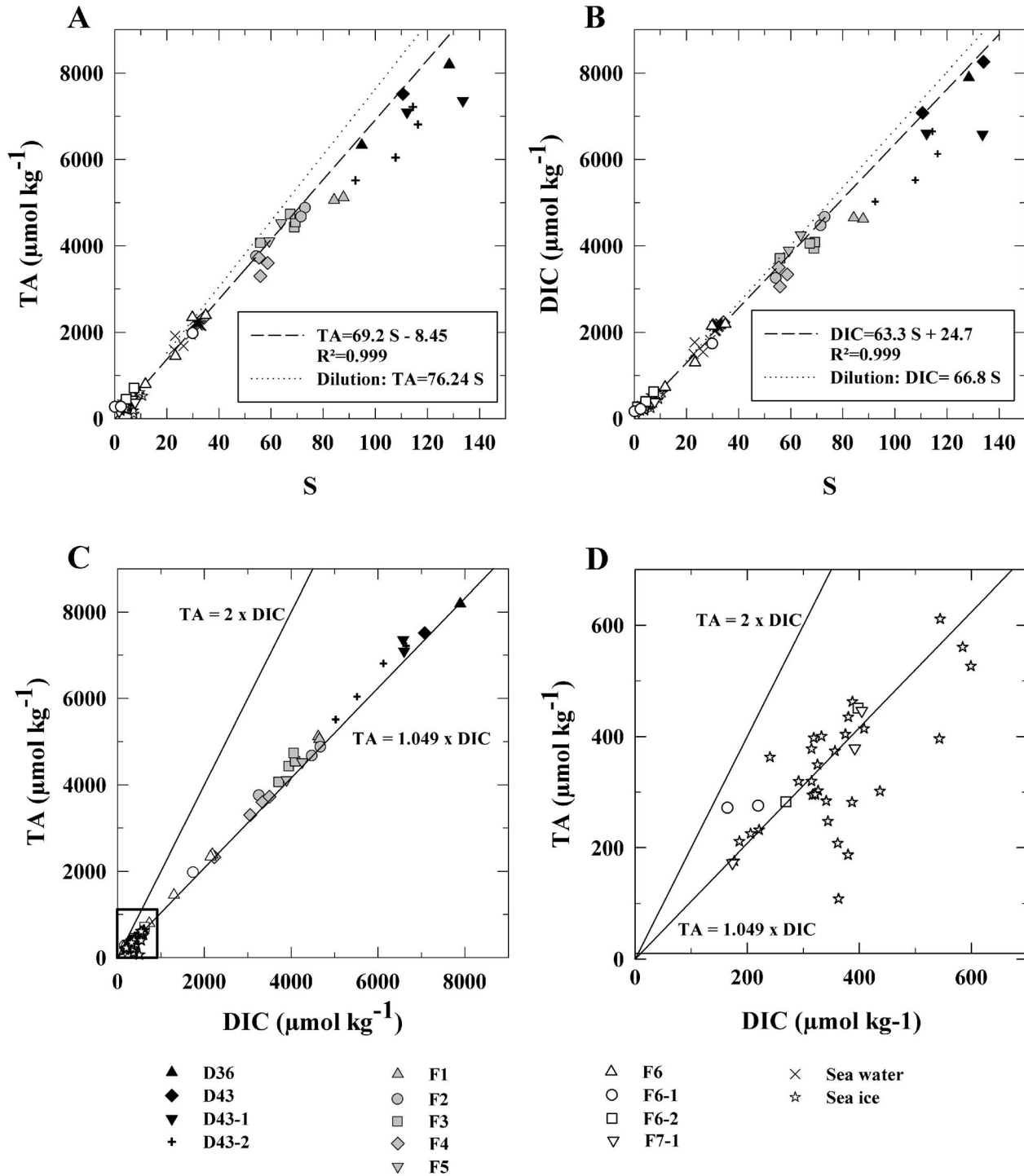


**Figure 6.** (a) TA and (b) DIC relationship with salinity of brine and seawater samples for all the CFL stations considered. The dotted line represents expected values based on dilution effect during melting while the dashed line represents the highly correlated relation between TA (or DIC) with salinity. (c) The relation between TA and DIC for both the brine and the sea ice (stars) is shown. (d) A “zoom in” of the square from Figure 6c in order to better document the relation in bulk sea ice. The two lines show the ratio TA: DIC of 2 (representing the stoichiometry of the precipitation/dissolution equilibrium in equation (1)) and the TA: DIC ratio of 1.049, typical of the underlying seawater.

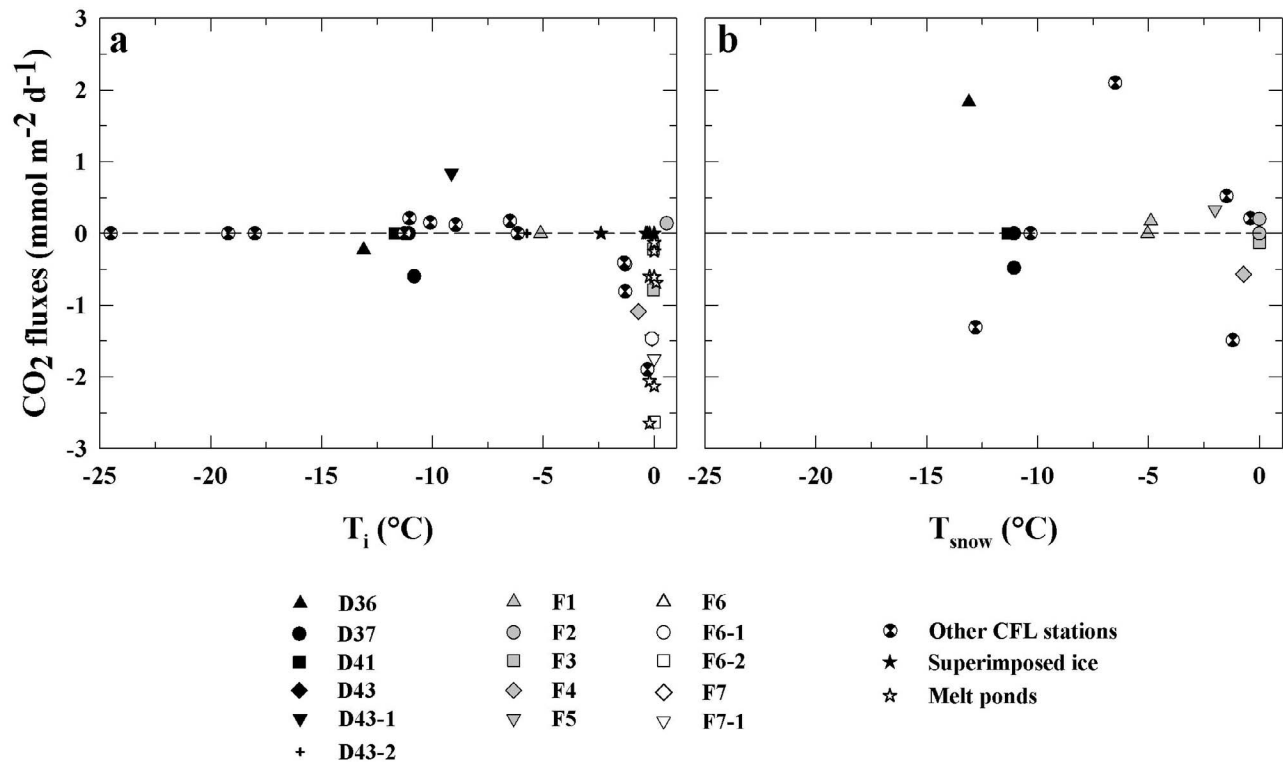


**Figure 7.** CO<sub>2</sub> fluxes measured on sea ice, melt ponds and superimposed ice interface (a) with the atmosphere and (b) on the snow. The other CFL stations represent additional sampling stations where only fluxes were measured.

rapid decrease of DIC at the bottom of the ice, as reported by *Shadwick et al.* [2011]. This sympagic bloom led to a sharp increase of net community production in the surface water up to 1.1 mol C m<sup>-2</sup> month<sup>-1</sup> [*Shadwick et al.*, 2011]. However, in June, Chl a concentration decreased significantly down to 1 μg L<sup>-1</sup>, likely due to brine flushing. This range of Chl a concentration was also observed at the bottom of the ice cover by *Song et al.* [2011] and *Mundy et al.* [2011]. At that time brine pCO<sub>2</sub> continued to decrease, suggesting that processes other than the production of sympagic algae contributed to the pCO<sub>2</sub> decrease. Thereafter, the impact of primary production on pCO<sub>2</sub> appears to last only a few weeks during biomass build up prior to brine flushing.

#### 4.2. Effects of CaCO<sub>3</sub> Precipitation, Dissolution

[33] As suggested by *Rysgaard et al.* [2009, 2007] and *Delille* [2006], other processes, such as CaCO<sub>3</sub> dissolution, can potentially promote the decrease in brine pCO<sub>2</sub>. According to equations (1)–(3), CaCO<sub>3</sub> precipitation reduces both DIC and TA in the brine. *Rysgaard et al.* [2007] suggested that this precipitation within sea ice could drive significant CO<sub>2</sub> uptake and that the TA: DIC ratio as high as 2 in melted bulk sea ice indicates that CaCO<sub>3</sub> precipitation occurs. During our survey, brine samples with salinity larger than 80 showed lower TA and DIC than expected from salinity changes (Figures 6a and 6b). In addition, plotting TA<sub>35</sub> as a function of DIC<sub>35</sub> (TA and DIC values being normalized to a salinity of 35 to discard concentration/dilution effects) indicates that these high salinity brine samples (D36, D43–1, D43–2, F1, F3, and F4) are well

aligned (slope 0.89, R<sup>2</sup> > 0.999) on a trend between the theoretical trend for calcium carbonate precipitation and the one for CO<sub>2</sub> degassing (Figure 8). This could be expected if both CaCO<sub>3</sub> precipitations occurred in high salty brines and CO<sub>2</sub> degassing occurred in the sea ice (Figure 8). This is consistent with previous findings of *Rysgaard et al.* [2007].

[34] In order to compare with literature, we computed none-normalized TA: DIC ratio in bulk ice that is about 0.96 (Figures 6c and 6d), i.e., very close to the value of underlying water (1.049) and the value of 1.01 reported by *Miller et al.* [2011], but significantly lower than the average of values reported by *Rysgaard et al.* [2007] in Franklin Bay that is about 1.55. *Miller et al.* [2011] addressed discrepancies between their study and observations of *Rysgaard et al.* [2007] and proposed several explanations. *Miller et al.* [2011] suggested that brines could be lost during the transport to the ship, which could not be possible in this study as the ice was vacuum-packed in the field, directly after the ice sampling. It is also suggested that an incomplete CaCO<sub>3</sub> dissolution could have a significant impact as the spatial variability.

[35] TA<sub>35</sub> and DIC<sub>35</sub> of bulk ice are lower than TA<sub>35</sub> and DIC<sub>35</sub> from the underlying water as a result of CaCO<sub>3</sub> precipitation and subsequent release of by-products of CaCO<sub>3</sub> into the water column (Figure 8).

#### 4.3. Effects of Temperature and Salinity

[36] As the ice temperature increases, ice crystals melt and salinity decreases accordingly. We explored the relationships among brine pCO<sub>2</sub>, temperature and salinity according

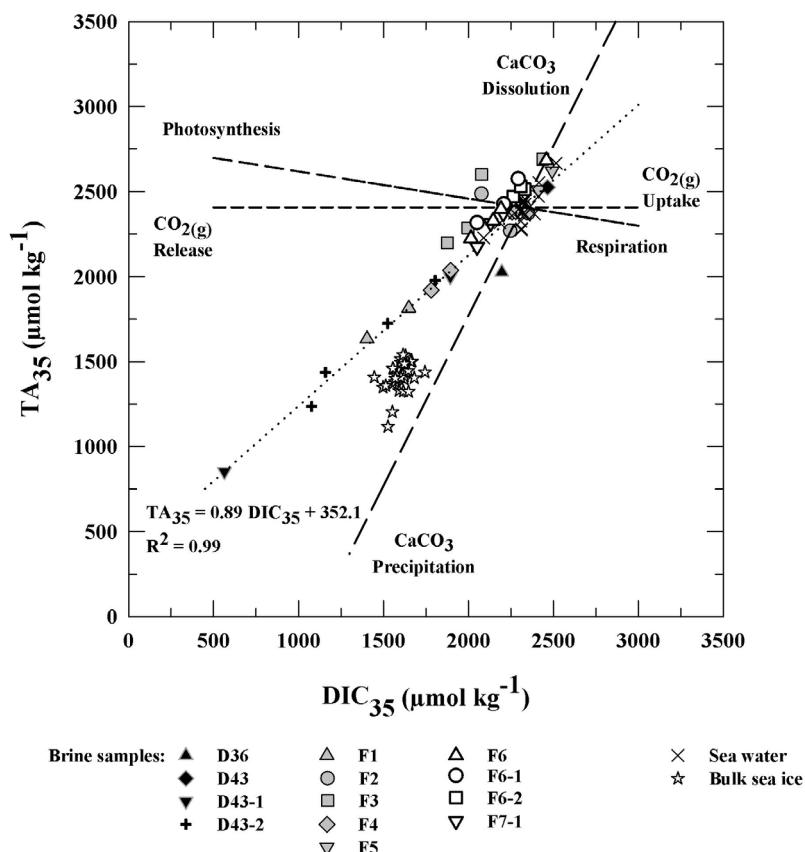


**Figure 8.** DIC<sub>35</sub>: TA<sub>35</sub> (values normalized to a salinity of 35) relationship in brine, seawater samples and ice samples. The different dotted lines represent the theoretical evolution of DIC<sub>35</sub>: TA<sub>35</sub> following a precipitation/dissolution of calcium carbonate, a release or uptake of CO<sub>2(g)</sub> and impacts of biology.

to the following steps: (i) we calculated brine salinity at a given temperature according to the relationship of *Cox and Weeks* [1983]; (ii) we normalized mean TA and DIC to a salinity of 35 (TA<sub>35</sub>, and DIC<sub>35</sub>, respectively) for all samples with salinity <80 (see section 4.2 for the choice of this threshold); (iii) we computed TA<sub>*t*</sub> and DIC<sub>*t*</sub> at a given temperature, *t* (and related salinity) assuming a conservative behavior of TA and DIC; and (iv) computed the brine pCO<sub>2</sub> for each temperature from TA<sub>*t*</sub> and DIC<sub>*t*</sub>, using CO2SYS [Lewis and Wallace, 1998] with the CO<sub>2</sub> acidity constants of *Dickson and Millero* [1987]. Here we assume that these constants are valid for the range of temperatures and salinities encountered within the sea ice [Delille *et al.*, 2007; Papadimitriou *et al.*, 2004]. The resulting pCO<sub>2</sub> - temperature relationship (denoted as CFL-dilution) is shown in Figure 9. A test of root mean square deviation was carried out on the dilution curve and showed a mean dispersion of 230 μatm. This dispersion decreased in June down to 52 μatm. Scattering is due to spatial heterogeneity, superimposition of physical and biogeochemical processes that are not related together, and thermal history of the ice, among other explanations.

[37] The observed pCO<sub>2</sub> response to temperature, roughly mimics the dilution curve, highlighting a major control of melting on pCO<sub>2</sub> as observed in Antarctica by *Delille* [2006] and coworkers. In June, brine drainage significantly reduced bulk ice salinity, leading to a drastic decrease in pCO<sub>2</sub>, down

to the almost zero as a result of the melting of low-CO<sub>2</sub> pure ice matrix.

#### 4.4. Under-Ice Melt Ponds

[38] Ice melting, brine flushing, and drainage of melt pond lead to the formation of a stable fresh water layer at the ice-ocean interface. These fresh water lenses, called under-ice melt ponds by *Hanson* [1965], are usually trapped under thinner ice areas or in depressions in the bottom of thicker ice. Within this fresh water layer, we observed a marked undersaturation down to 5 μatm (Figure 4c). At that time, despite the increase in light availability, algal biomass remained low, probably as a consequence of nitrate + nitrite limitation [Mundy *et al.*, 2011]. Our results suggest that phytoplanktonic growth can also be limited by CO<sub>2</sub> availability as already suggested by *Wolf-Gladrow and Riebesell* [1997] and *Riebesell et al.* [1993]. Hence, phytoplanktonic limited growth is likely to play a minor role on CO<sub>2</sub> undersaturation. At that time pCO<sub>2</sub> of melt ponds at the top of the ice was larger than pCO<sub>2</sub> of under-ice melt ponds, suggesting that this low salinity-low pCO<sub>2</sub> water layer is originated from melted sea ice, rather than surface melt ponds that percolated through the ice.

#### 4.5. Inter-Hemisphere Comparison

[39] In Antarctica, *Delille* [2006] and coworkers reported values of brine pCO<sub>2</sub> ranging from 30 μatm to 920 μatm.

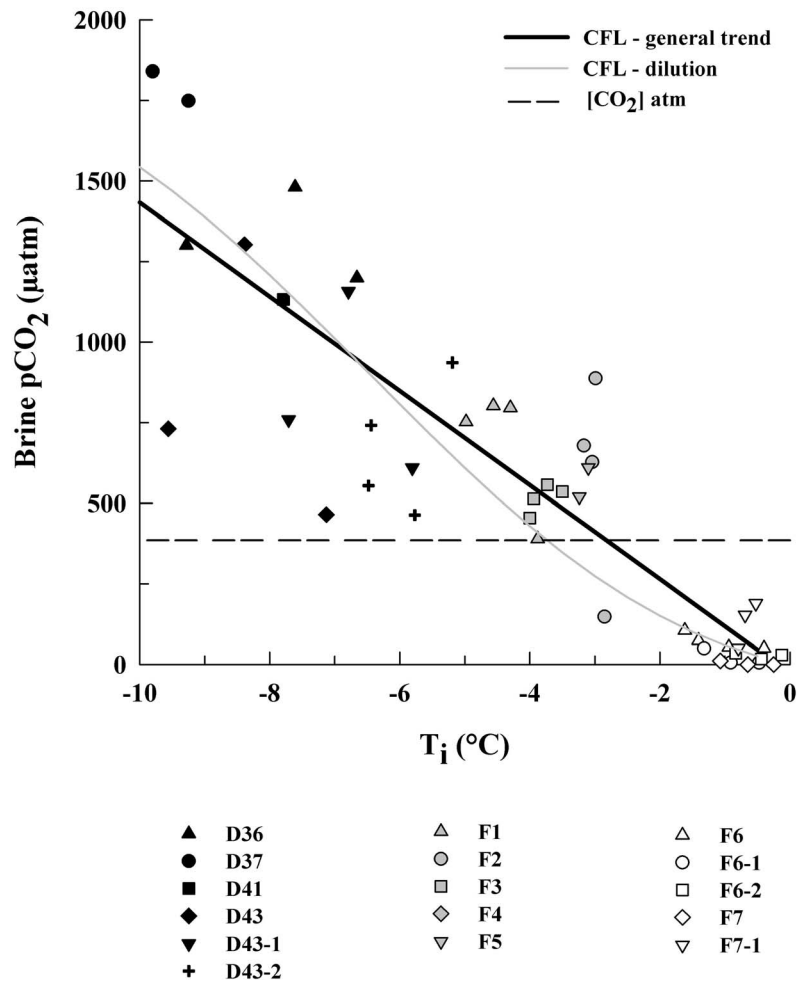


**Figure 9.** Evolution of the direct in situ brine pCO<sub>2</sub> measurements with the ice temperature ( $T_i$ ). The ice temperature was integrated over the depth of ice where the brine was sampled (i.e., from surface to bottom of sackholes). The black line represents the general trend during CFL while the gray line represents the pCO<sub>2</sub>: temperature relationship computed (from TA and DIC) for the dilution effect (see text for details) and the dotted line represents the atmospheric CO<sub>2</sub> concentration.

The range of pCO<sub>2</sub> observed during the survey was significantly larger than in Antarctica, with both higher and lower end values (Figure 9). In cold sea ice in particular, we observed significantly higher pCO<sub>2</sub> values in the Amundsen Gulf than in the Antarctic for a given temperature. As discussed above, several processes can be responsible for the pCO<sub>2</sub> dynamics within the sea ice brine: temperature and salinity changes, calcium carbonate precipitation, and/or primary production. The first is unlikely to explain our Arctic-Antarctic discrepancies in cold sea ice. Also, at a given temperature, the effect of brine concentration on pCO<sub>2</sub> is expected to be similar in both hemispheres. The processes driving CaCO<sub>3</sub> precipitation in the brine network are also likely to be similarly controlled by temperature-driven brine concentration in sea ice from both polar regions. The discrepancy in pCO<sub>2</sub> between the polar regions may be related to differences in the rate that organic carbon is oxidized through ecosystem respiration.

[40] We compared organic matter (dissolved organic carbon, DOC, and particulate organic carbon, POC) abundance

in the Amundsen Gulf and Antarctic open water (Table 2). Higher level of organic matter in the Amundsen Gulf, compared to Antarctic open waters is likely due to large riverine input. The Mackenzie River, the largest river in terms of POC discharge in the Arctic, has the potential to cause strong variations in POC export from shelf to basin, and discharge directly in the Beaufort Sea [Lalonde *et al.*, 2009]. According to Magen *et al.* [2010], the Mackenzie River mainly contributes to the input of organic matter. Higher organic carbon concentration in the Amundsen Gulf compared to the Antarctic could potentially support higher respiration and related CO<sub>2</sub> production and can therefore possibly explain the generally higher pCO<sub>2</sub> values. Taking into account that the Arctic Ocean is a closed sea with a stronger continental organic matter input compared to the Antarctic, elevated pCO<sub>2</sub> in cold sea ice could be a general feature in the Arctic. More pCO<sub>2</sub> surveys in the Arctic sea ice and reliable assessment of winter respiration over the whole ice thickness is however required to settle this question. We can note that terrestrial DOC transport into the Arctic Ocean can

**Table 2.** POC and DOC Concentration in Sea Ice<sup>a</sup>

	Location	POC ( $\mu\text{mol L}^{-1}$ )	DOC ( $\mu\text{mol L}^{-1}$ )
<i>Arctic</i>			
Riedel et al. [2008]	Pre-bloom	53.53	60.22
	Bloom	740.54	496.29
	Post-bloom	2185.93	777.34
Song et al. [2011]			563 $\pm$ 434
<i>Antarctic</i>			
Dumont [2009]	Bruxelles	35.34	55.2
	Liège	26.6	34.2
Thomas et al. [2001]	SE Weddell Sea		523
	Bellingshausen Sea		109
	Weddell Sea		207

<sup>a</sup>In Arctic, Riedel et al. [2008] measured POC and DOC concentration in the bottom 4 cm of the ice from February 24 to June 20 in Franklin Bay, in the Amundsen Gulf in the frame of the *Canadian Arctic Shelf Exchanges Study* (CASES). Song et al. [2011] measured DOC concentration in the bottom 10 cm of the ice between mid-March and early July 2008. Dumont [2009] measured POC and DOC within sea ice in the Bellingshausen Sea, Antarctica in September–October 2007. Thomas et al. [2001] presented data from the southeastern Weddell Sea in April–May 1992, Bellingshausen Sea in January–February 1994 and Weddell Sea in January–March 1997. Data from Dumont [2009] are an average on the bottom 10 cm of the ice, while Thomas et al. [2001] only shows mean values.

potentially change as a consequence of global change [Alling et al., 2010]. This can affect sea ice pCO<sub>2</sub> inter-hemispheric differences due to organic matter respiration.

#### 4.6. Air-Ice CO<sub>2</sub> Fluxes

[41] In cold sea ice (below  $-11^{\circ}\text{C}$ ) we did not detect significant air-ice CO<sub>2</sub> fluxes. As temperature increased, ice became permeable to gases, and air-CO<sub>2</sub> fluxes were observed for temperature above  $-11^{\circ}\text{C}$ . Effluxes of CO<sub>2</sub> from the ice to the atmosphere were then observed in April (Figure 7) while brine pCO<sub>2</sub> was supersaturated with respect to the atmosphere, which explains the decrease of the brine pCO<sub>2</sub> observed in the top layers in the vertical profiles of Figure 5. In some cases we observed CO<sub>2</sub> effluxes while brine volume was under the permeability threshold of 5% [Golden et al., 2007]. According to Loose et al. [2011] and Gosink et al. [1976], the porosity threshold for gas transport may be lower than for fluid transport [Golden et al., 2007]. If the gas transport threshold is lower than the threshold of permeability for liquid, then diffusive transport could allow gas exchanges earlier in the spring and later in the fall or even during winter. However, further experiments are needed to better explain and constrain gas fluxes below the permeability threshold for liquids.

[42] In addition, the internal precipitation of calcium carbonate at that time or earlier could promote the release of CO<sub>2</sub> to the atmosphere. This is consistent with the observed trend of the DIC<sub>35</sub>: TA<sub>35</sub> relationship in the high salinity brine sample that suggests a release of CO<sub>2</sub> associated with the precipitation of CaCO<sub>3</sub> (Figure 8). From May, the brine pCO<sub>2</sub> were initially supersaturated but decreased with rising ice temperature and passed below the threshold of the atmospheric concentration. Accordingly, negative fluxes were measured from station F6 onwards down to  $-2.6 \text{ mmol m}^{-2} \text{ d}^{-1}$ .

[43] This is in agreement with previous works of Nomura et al. [2010a, 2006] and Delille [2006], who suggested that brine pCO<sub>2</sub> is an important factor controlling the air-ice CO<sub>2</sub>

flux. The magnitude of CO<sub>2</sub> fluxes also depends on sea ice permeability. Since ice temperature controls both pCO<sub>2</sub> and permeability through brine volume [Golden et al., 2007], ice temperature therefore appears to be one of the main control of air-ice CO<sub>2</sub> fluxes.

[44] Air-ice CO<sub>2</sub> fluxes are also affected by the state of the air-ice interface. A particular importance is the occurrence of superimposed ice that clearly impedes air-ice gas transfer (Figure 7a). Nomura et al. [2010a] suggested that snow cover was an impermeable medium, blocking CO<sub>2</sub> diffusion and exchange to the atmosphere. Nevertheless, this observation was made during superimposed ice formation [Nomura et al., 2010b]. Our observations agree with the work of Nomura et al. [2010b] and Delille [2006], suggesting that superimposed ice hamper air-ice CO<sub>2</sub> fluxes. However, in none-superimposed ice conditions, we observed CO<sub>2</sub> fluxes as previously reported over snow covered terrestrial ecosystem. In our study, air-ice CO<sub>2</sub> fluxes appear to be driven by air-ice pCO<sub>2</sub> gradient and controlled by sea ice permeability. Air-ice fluxes appear to be moderated by the snow, but the CO<sub>2</sub> fluxes measured in absence of snow do not translate readily into snow-air CO<sub>2</sub> fluxes. Snow physical and chemical properties, e.g., porosity, texture, salinity, total alkalinity, among other parameters like snow thickness, are likely to affect the magnitude of the fluxes. The impact of the snow cover on gas exchanges is still unknown. Albert et al. [2002] suggested that the high permeability of the snowpack allow rapid gases exchanges with the atmosphere, even with moderate winds. On the other hand, Takagi et al. [2005] found that CO<sub>2</sub> concentrations in the snowpack fluctuated significantly as wind speed varied suggesting a strong wind-pumping effect on CO<sub>2</sub> movement in the snowpack. Using eddy covariance, Papakyriakou and Miller [2011] generally found fluxes to increase with increasing wind speed over seasonal sea ice, with the largest fluxes occurring during periods of blowing snow.

[45] By contrast, melt ponds development appears to promote the uptake of CO<sub>2</sub> by the ice with observed air-ice CO<sub>2</sub> fluxes as low as  $-2.7 \text{ mmol m}^{-2} \text{ d}^{-1}$ . This magnitude is lower than what was reported by Nomura et al. [2010a] with values ranging from  $-38.6 \text{ mmol m}^{-2} \text{ d}^{-1}$  to  $-19.5 \text{ mmol m}^{-2} \text{ d}^{-1}$  over melt ponds in landfast ice near Barrow, Alaska. These fluxes are in the same order of magnitude as fluxes measured by Semiletov et al. [2004] using the chamber and eddy correlation techniques. Semiletov et al. [2004] suggested a significant role of photosynthesis activity to the fluxes. However, Chl a was measured on melt ponds and exhibited low concentration ( $\sim 2 \mu\text{g L}^{-1}$ ) as also measured by Mundy et al. [2011]. On the other hand, melting of low-CO<sub>2</sub> pure ice matrix acts to decrease pCO<sub>2</sub>.

[46] We attempted to assess the potential uptake of atmospheric CO<sub>2</sub> by melting sea ice that equilibrates with the atmosphere. In the station F6–2, we observed air-ice CO<sub>2</sub> fluxes around  $-2.6 \text{ mmol m}^{-2} \text{ d}^{-1}$ . Taking into account the brine conditions (TA =  $451 \mu\text{mol kg}^{-1}$ , DIC =  $398 \mu\text{mol kg}^{-1}$ , S = 4.4 and T =  $-0.8^{\circ}\text{C}$ ), the equilibrium of such brines with the atmosphere (pCO<sub>2</sub> =  $390 \mu\text{atm}$ ) would correspond to an uptake of CO<sub>2</sub> of  $80 \mu\text{mol kg}^{-1}$  of brines. In the same way, the equilibration of ice samples of station F6–2, or pure freshwater ice would correspond to an uptake of 40 and  $32 \mu\text{mol kg}^{-1}$  of ice respectively. If we assume a complete melting and subsequent equilibrium with the atmosphere of

a 1.3 m thick ice cover within one month, this would lead to average CO<sub>2</sub> fluxes ranging from  $-1.2$  to  $-3.1$  mmol m<sup>-2</sup> d<sup>-1</sup> that are rather consistent with the air-ice CO<sub>2</sub> fluxes measured over melt ponds and decaying sea ice ( $-0.02$  mmol m<sup>-2</sup> d<sup>-1</sup> to  $-2.65$  mmol m<sup>-2</sup> d<sup>-1</sup>). This computation provides a potential CO<sub>2</sub> uptake, assuming an ideal case of complete melting without interactions with the underlying seawater.

## 5. Conclusions

[47] This study gives an overview of the evolution of pCO<sub>2</sub> dynamics within sea ice from late spring to summer in the Arctic coastal waters of the Amundsen Gulf. We present the first vertical profiles of pCO<sub>2</sub> in sea ice brine to demonstrate the evolution with the physical and biogeochemical parameters in the ice and their relationship to the CO<sub>2</sub> fluxes at the ice-atmosphere interface.

[48] As sea ice forms and grows, and ice temperature decreases, all the impurities (including salts, organic matter and gases) are concentrated in brine leading to a significant increase of brine salinity and brine pCO<sub>2</sub> (up to 1839 μatm in April). As salinity increases, significant changes with respect to mineral-liquid thermodynamic equilibrium can occur and calcium carbonate can precipitate [Dieckmann *et al.*, 2008]. Indirect evidence of such precipitation was observed within highly saline brine, in the upper part of the sea ice cover and in bulk sea ice. This is in agreement with the work of Dieckmann *et al.* [2008] and Rysgaard *et al.* [2009, 2007].

[49] As summer draws near, the ice temperature increases and, according to Delille *et al.* [2007], Delille [2006], Nomura *et al.* [2006], and Papadimitriou *et al.* [2004], the brine pCO<sub>2</sub> decreases. We measured a shift from 1834 μatm in April to almost 0 μatm in June. This decrease was mainly due to the brine dilution by fresh water coming from internal and surface melting of sea ice. Dissolution of calcium carbonate and primary production enhance this spring/summer pCO<sub>2</sub> decrease. As sea ice became more permeable to gas exchange and brine became undersaturated, strong negative CO<sub>2</sub> fluxes were observed (down to  $-2.6$  mmol m<sup>-2</sup> d<sup>-1</sup> above sea ice and  $-2.7$  mmol m<sup>-2</sup> d<sup>-1</sup> above melt ponds).

[50] While primary production at the bottom of the ice reduces the brine pCO<sub>2</sub> during spring bloom, organic matter degradation by microbial communities could explain the higher pCO<sub>2</sub> level in the Amundsen Gulf compared to Antarctic open waters in winter.

[51] **Acknowledgments.** The authors would like to acknowledge the outstanding support and kindness of the crew members of the *CCGS Amundsen*. We would like to also thank Jens Ehn for his strong and crucial help during the all CFL cruise. Funding for the CFL project was provided by the Canadian International Year (IPY) program office, the Canadian Natural Sciences and Engineering Research Council (NSERC), ArcticNet - a Network of Centres of Excellence, the Canada Research Chairs (CRC) Program and the Canada Foundation for Innovation (CFI). We would also like to thank Ms. Noel from NGI (Belgium) for her support in mapping. This research was also supported by the F.R.S-FNRS (contract 2.4649.07), with which BD is a research associate, and the Belgian Science Policy (contract SD/CA/03A). NXG received a PhD grant from the Fonds pour la Formation à la Recherche dans l'Industrie et l'Agriculture. This is MARE contribution 222.

## References

Albert, M. R., A. M. Grannas, J. Bottenheim, P. B. Shepson, and F. E. Perron (2002), Processes and properties of snow-air transfer in the high Arctic

- with application to interstitial ozone at Alert, Canada, *Atmos. Environ.*, 36(15–16), 2779–2787, doi:10.1016/S1352-2310(02)00118-8.
- Alling, V., et al. (2010), Nonconservative behavior of dissolved organic carbon across the Laptev and East Siberian seas, *Global Biogeochem. Cycles*, 24, GB4033, doi:10.1029/2010GB003834.
- Anderson, L. G., E. Falck, E. P. Jones, S. Jutterstrom, and J. H. Swift (2004), Enhanced uptake of atmospheric CO<sub>2</sub> during freezing of seawater: A field study in Storfjorden, Svalbard, *J. Geophys. Res.*, 109, C06004, doi:10.1029/2003JC002120.
- Arrigo, K. R., and D. N. Thomas (2004), Large scale importance of sea ice biology in the Southern Ocean, *Antarct. Sci.*, 16(4), 471–486, doi:10.1017/S0954102004002263.
- Arrigo, K. R., T. Mock, and P. M. Lizotte (2010), Primary producers and sea ice, in *Sea Ice*, 2nd ed., pp. 283–326, Wiley-Blackwell, Oxford, U. K.
- Bates, N. R., and J. T. Mathis (2009), The Arctic Ocean marine carbon cycle: Evaluation of air-sea CO<sub>2</sub> exchanges, ocean acidification impacts and potential feedbacks, *Biogeosciences*, 6(11), 2433–2459, doi:10.5194/bg-6-2433-2009.
- Cai, W.-J., et al. (2010), Decrease in the CO<sub>2</sub> uptake capacity in an ice-free Arctic Ocean basin, *Science*, 329(5991), 556–559, doi:10.1126/science.1189338.
- Comiso, J. C. (2003), Large-scale characteristics and variability of the global sea ice cover, in *Sea Ice: An Introduction to Its Physics, Chemistry, Biology and Geology*, pp. 112–142, Blackwell Sci., London.
- Copin Montégut, C. (1988), A new formula for the effect of temperature on the partial pressure of carbon dioxide in seawater, *Mar. Chem.*, 25, 29–37, doi:10.1016/0304-4203(88)90012-6.
- Cox, G. F. N., and W. F. Weeks (1983), Equations for determining the gas and brine volumes in sea-ice samples, *J. Glaciol.*, 29(102), 306–316.
- Delille, B. (2006), Inorganic carbon dynamics and air-ice-sea CO<sub>2</sub> fluxes in the open and coastal waters of the Southern Ocean, PhD thesis, 296 pp., Univ. de Liège, Liège, France.
- Delille, B., B. Jourdain, A. V. Borges, J. L. Tison, and D. Delille (2007), Biogas (CO<sub>2</sub>, O<sub>2</sub>, dimethylsulfide) dynamics in spring Antarctic fast ice, *Limnol. Oceanogr.*, 52(4), 1367–1379, doi:10.4319/lo.2007.52.4.1367.
- Dickson, A. G., and F. J. Millero (1987), A comparison of the equilibrium constants for the dissociation of carbonic acid in seawater media, *Deep-Sea Res.*, 34, 1733–1743, doi:10.1016/0198-0149(87)90021-5.
- Dickson, A. G., C. L. Sabine, and J. R. Christian (2007), Guide to best practices for ocean CO<sub>2</sub> measurements, *PICES Spec. Publ.*, 3, 1–191.
- Dieckmann, G. S., and H. H. Hellmer (2010), The importance of sea ice: An overview, in *Sea Ice: An Introduction to its Physics, Chemistry, Biology and Geology*, 2nd ed., edited by D. N. Thomas and G. S. Dieckmann, pp. 1–22, Blackwell Sci., Oxford, U. K.
- Dieckmann, G. S., G. Nehrke, S. Papadimitriou, J. Gottlicher, R. Steininger, H. Kennedy, D. Wolf-Gladrow, and D. N. Thomas (2008), Calcium carbonate as ikaite crystals in Antarctic sea ice, *Geophys. Res. Lett.*, 35, L08501, doi:10.1029/2008GL033540.
- Dieckmann, G. S., G. Nehrke, C. Uhlig, J. Göttlicher, S. Gerland, M. A. Granskog, and D. N. Thomas (2010), Brief communication: Ikaite (CaCO<sub>3</sub>·6H<sub>2</sub>O) discovered in Arctic sea ice, *The Cryosphere*, 4, 227–230, doi:10.5194/tc-4-227-2010.
- Dumont, I. (2009), Interactions between the microbial network and the organic matter in the Southern Ocean: Impacts on the biological carbon pump, PhD thesis, 202 pp., Univ. Libre de Bruxelles, Brussels.
- Eicken, H. (2003), From the microscopic to the macroscopic to the regional scale, growth, microstructure and properties of sea ice, in *Sea Ice: An Introduction to Its Physics, Biology, Chemistry and Geology*, pp. 22–81, Blackwell Sci., London.
- Frankignoulle, M. (1988), Field-measurements of air sea CO<sub>2</sub> exchange, *Limnol. Oceanogr.*, 33(3), 313–322, doi:10.4319/lo.1988.33.3.0313.
- Fransson, A., M. Chierici, and Y. Nojiri (2009), New insights into the spatial variability of the surface water carbon dioxide in varying sea ice conditions in the Arctic Ocean, *Cont. Shelf Res.*, 29, 1317–1328, doi:10.1016/j.csr.2009.03.008.
- Gibson, J. A. E., and T. W. Trull (1999), Annual cycle of fCO<sub>2</sub> under sea-ice and in open water in Prydz Bay, East Antarctica, *Mar. Chem.*, 66, 187–200, doi:10.1016/S0304-4203(99)00040-7.
- Gleitz, M., et al. (1995), Comparison of summer and winter inorganic carbon, oxygen and nutrient concentrations in Antarctic sea ice brine, *Mar. Chem.*, 51, 81–91, doi:10.1016/0304-4203(95)00053-T.
- Golden, K. M., H. Eicken, A. L. Heaton, J. Miner, D. J. Pringle, and J. Zhu (2007), Thermal evolution of permeability and microstructure in sea ice, *Geophys. Res. Lett.*, 34, L16501, doi:10.1029/2007GL030447.
- Gosink, T. A., J. G. Pearson, and J. J. Kelly (1976), Gas movement through sea ice, *Nature*, 263, 41–42, doi:10.1038/263041a0.
- Hanson, A. M. (1965), Studies of the mass budget of arctic pack-ice floes, *J. Glaciol.*, 5(41), 701–709.

- Heinesch, B., M. Yernaux, M. Aubinet, N. X. Geilfus, T. Papakyriakou, G. Carnat, H. Eicken, J. L. Tison, and B. Delille (2009), Measuring air-ice CO<sub>2</sub> fluxes in the Arctic, *FluxLetter*, 2, 9–10.
- Intergovernmental Panel on Climate Change (2007), Climate Change 2007: Intergovernmental Panel on Climate Change Fourth Assessment Report, Geneva, Switzerland.
- Johnson, K. M., K. D. Wills, D. B. Butler, W. K. Johnson, and C. S. Wong (1993), Coulometric total carbon dioxide analysis for marine studies—Maximizing the performance of an automated gas extraction system and coulometric detector, *Mar. Chem.*, 44, 167–187, doi:10.1016/0304-4203(93)90201-X.
- Killawee, J. A., I. J. Fairchild, J. L. Tison, L. Janssens, and R. Lorrain (1998), Segregation of solutes and gases in experimental freezing of dilute solutions: Implications for natural glacial systems, *Geochim. Cosmochim. Acta*, 62(23–24), 3637–3655, doi:10.1016/S0016-7037(98)00268-3.
- Lalande, C., A. Forest, D. G. Barber, Y. Gratton, and L. Fortier (2009), Variability in the annual cycle of vertical particulate organic carbon export on Arctic shelves: Contrasting the Laptev Sea, northern Baffin Bay and the Beaufort Sea, *Cont. Shelf Res.*, 29, 2157–2165, doi:10.1016/j.csr.2009.08.009.
- Lewis, E., and D. W. R. Wallace (1998), Program developed for CO<sub>2</sub> system calculations, *Rep. ORNL/CDLAC-105*, Carbon Dioxide Inf. Anal. Cent., Oak Ridge Natl. Lab., Oak Ridge, Tenn.
- Loose, B., P. Schlosser, D. Perovich, D. Ringelberg, D. T. Ho, T. Takahashi, J. Richter-Menge, C. M. Reynolds, W. R. McGillis, and J. L. Tison (2011), Gas diffusion through columnar laboratory sea ice: Implications for mixed-layer ventilation of CO<sub>2</sub> in the seasonal ice zone, *Tellus, Ser. B*, 63(1), 23–39, doi:10.1111/j.1600-0889.2010.00506.x.
- Magen, C., G. Chaillou, S. A. Crowe, A. Mucci, B. Sundby, A. G. Gao, R. Makabe, and H. Sasaki (2010), Origin and fate of particulate organic matter in the southern Beaufort Sea—Amundsen Gulf region, Canadian Arctic, *Estuarine Coastal Shelf Sci.*, 86(1), 31–41, doi:10.1016/j.ecss.2009.09.009.
- Marion, G. M. (2001), Carbonate mineral solubility at low temperatures in the Na-K-Mg-Ca-H-Cl-SO<sub>4</sub>-OH-HCO<sub>3</sub>-CO<sub>3</sub>-CO<sub>2</sub>-H<sub>2</sub>O system, *Geochim. Cosmochim. Acta*, 65(12), 1883–1896, doi:10.1016/S0016-7037(00)00588-3.
- Miller, L., T. Papakyriakou, R. E. Collins, J. Deming, J. Ehn, R. W. Macdonald, A. Mucci, O. Owens, M. Raudsepp, and N. Sutherland (2011), Carbon dynamics in sea ice: A winter flux time series, *J. Geophys. Res.*, 116, C02028, doi:10.1029/2009JC006058.
- Mundy, C. J., et al. (2011), Characteristics of two distinct high-light acclimated algal communities during advanced stages of sea ice melt, *Polar Biol.*, 34(12), 1869–1886.
- Munro, D. R., R. B. Dunbar, D. A. Mucciarone, K. R. Arrigo, and M. C. Long (2010), Stable isotope composition of dissolved inorganic carbon and particulate organic carbon in sea ice from the Ross Sea, Antarctica, *J. Geophys. Res.*, 115, C09005, doi:10.1029/2009JC005661.
- Nomura, D., H. Yoshikawa-Inoue, and T. Toyota (2006), The effect of sea-ice growth on air-sea CO<sub>2</sub> flux in a tank experiment, *Tellus, Ser. B*, 58(5), 418–426, doi:10.1111/j.1600-0889.2006.00204.x.
- Nomura, D., H. Eicken, R. Gradinger, and K. Shirasawa (2010a), Rapid physically driven inversion of the air-sea ice CO<sub>2</sub> flux in the seasonal landfast ice off Barrow, Alaska after onset surface melt, *Cont. Shelf Res.*, 30, 1998–2004, doi:10.1016/j.csr.2010.09.014.
- Nomura, D., H. Yoshikawa-Inoue, T. Toyota, and K. Shirasawa (2010b), Effects of snow, snow-melting and re-freezing processes on air-sea ice CO<sub>2</sub> flux, *J. Glaciol.*, 56, 262–270.
- Papadimitriou, S., H. Kennedy, G. Kattner, G. S. Dieckmann, and D. N. Thomas (2004), Experimental evidence for carbonate precipitation and CO<sub>2</sub> degassing during sea ice formation, *Geochim. Cosmochim. Acta*, 68(8), 1749–1761, doi:10.1016/j.gca.2003.07.004.
- Papadimitriou, S., D. N. Thomas, H. Kennedy, C. Haas, H. Kuosa, A. Krell, and G. S. Dieckmann (2007), Biogeochemical composition of natural sea ice brines from the Weddell Sea during early austral summer, *Limnol. Oceanogr.*, 52(5), 1809–1823, doi:10.4319/lo.2007.52.5.1809.
- Papakyriakou, T., and L. Miller (2011), Springtime CO<sub>2</sub> exchange over seasonal sea ice in the Canadian Arctic Archipelago, *Ann. Glaciol.*, 52(57), 215–224, doi:10.3189/172756411795931534.
- Parsons, T. R., Y. Maita, and C. M. Lalli (1984), *A Manual of Chemical and Biological Methods for Seawater Analysis*, 173 pp., Pergamon, Toronto, Ont., Canada.
- Riebesell, U., D. A. Wolf-Gladrow, and V. Smetacek (1993), Carbon dioxide limitation of marine phytoplankton growth rates, *Nature*, 361, 249–251, doi:10.1038/361249a0.
- Riedel, A., C. Michel, M. Gosselin, and B. LeBlanc (2008), Winter-spring dynamics in sea-ice carbon cycling in the coastal Arctic Ocean, *J. Mar. Syst.*, 74(3–4), 918–932, doi:10.1016/j.jmarsys.2008.01.003.
- Rysgaard, S., R. N. Glud, M. K. Sejr, J. Bendtsen, and P. B. Christensen (2007), Inorganic carbon transport during sea ice growth and decay: A carbon pump in polar seas, *J. Geophys. Res.*, 112, C03016, doi:10.1029/2006JC003572.
- Rysgaard, S., J. Bendtsen, L. T. Pedersen, H. Ramlov, and R. N. Glud (2009), Increased CO<sub>2</sub> uptake due to sea ice growth and decay in the Nordic Seas, *J. Geophys. Res.*, 114, C09011, doi:10.1029/2008JC005088.
- Sabine, C. L., et al. (2004), The oceanic sink for anthropogenic CO<sub>2</sub>, *Science*, 305(5682), 367–371, doi:10.1126/science.1097403.
- Semiletov, I. P., A. Makshtas, S. I. Akasofu, and E. L. Andreas (2004), Atmospheric CO<sub>2</sub> balance: The role of Arctic sea ice, *Geophys. Res. Lett.*, 31, L05121, doi:10.1029/2003GL017996.
- Semiletov, I. P., I. Pipko, I. Repina, and N. E. Shakhova (2007), Carbonate chemistry dynamics and carbon dioxide fluxes across the atmosphere-ice-water interfaces in the Arctic Ocean: Pacific sector of the Arctic, *J. Mar. Syst.*, 66(1–4), 204–226, doi:10.1016/j.jmarsys.2006.05.012.
- Shadwick, E. H., et al. (2011), Seasonal variability of the inorganic carbon system in the Amundsen Gulf region of the southeastern Beaufort Sea, *Limnol. Oceanogr.*, 56(1), 303–322, doi:10.4319/lo.2011.56.1.0303.
- Song, G., H. Xie, C. Aubry, Y. Zhang, M. Gosselin, C. J. Mundy, B. Philippe, and T. N. Papakyriakou (2011), Spatiotemporal variations of dissolved organic carbon and carbon monoxide in first-year sea ice in the western Canadian Arctic, *J. Geophys. Res.*, 116, C00G05, doi:10.1029/2010JC006867.
- Takagi, K., M. Nomura, D. Ashiya, H. Takahashi, K. Sasa, Y. Fujinuma, H. Shibata, Y. Akibayashi, and T. Koike (2005), Dynamic carbon dioxide exchange through snowpack by wind-driven mass transfer in a conifer-broadleaf mixed forest in northernmost Japan, *Global Biogeochem. Cycles*, 19, GB2012, doi:10.1029/2004GB002272.
- Takahashi, T., et al. (2002), Global sea-air CO<sub>2</sub> flux based on climatological surface ocean pCO<sub>2</sub>, and seasonal biological and temperature effects, *Deep Sea Res., Part II*, 49(9–10), 1601–1622, doi:10.1016/S0967-0645(02)00003-6.
- Takahashi, T., et al. (2009), Climatological mean and decadal change in surface ocean pCO<sub>2</sub>, and net sea-air CO<sub>2</sub> flux over the global oceans, *Deep Sea Res., Part II*, 56(8–10), 554–577, doi:10.1016/j.dsr2.2008.12.009.
- Thomas, D. N., G. Kattner, R. Engbrodt, V. Giannelli, H. Kennedy, C. Haas, and G. S. Dieckmann (2001), Dissolved organic matter in Antarctic sea ice, in *Annals of Glaciology*, vol. 33, edited by M. O. Jeffries and H. Eicken, pp. 297–303, Int. Glaciol. Soc., Cambridge, U. K.
- Tison, J. L., C. Haas, M. M. Gowing, S. Sleewaegen, and A. Bernard (2002), Tank study of physico-chemical controls on gas content and composition during growth of young sea ice, *J. Glaciol.*, 48(161), 177–191, doi:10.3189/172756502781831377.
- Tison, J. L., A. Worby, B. Delille, F. Brabant, S. Papadimitriou, D. Thomas, J. de Jong, D. Lannuzel, and C. Haas (2008), Temporal evolution of decaying summer first-year sea ice in the western Weddell Sea, Antarctica, *Deep Sea Res., Part II*, 55(8–9), 975–987, doi:10.1016/j.dsr2.2007.12.021.
- Wolf-Gladrow, D., and U. Riebesell (1997), Diffusion and reactions in the vicinity of plankton: A refined model for inorganic carbon transport, *Mar. Chem.*, 59, 17–34, doi:10.1016/S0304-4203(97)00069-8.
- Zeebe, R. E., and D. Wolf-Gladrow (2001), *CO<sub>2</sub> in Seawater: Equilibrium, Kinetics, Isotopes*, Elsevier, Amsterdam.
- Zemmelink, H. J., B. Delille, J. L. Tison, E. J. Hints, L. Houghton, and J. W. H. Dacey (2006), CO<sub>2</sub> deposition over the multi-year ice of the western Weddell Sea, *Geophys. Res. Lett.*, 33, L13606, doi:10.1029/2006GL026320.

G. Carnat, B. Else, N.-X. Geilfus, and T. Papakyriakou, Center for Earth Observation Science, University of Manitoba, 470 Wallace Bldg., 125 Dysart Rd., Winnipeg, MB R3T 2N2, Canada. (geilfusn@cc.umanitoba.ca)

B. Delille, Unité d'Océanographie Chimique, Université de Liège, Allée du 6 août 17, B-4000 Liege, Belgium.

E. Shadwick, Center for Marine and Atmosphere Research, Commonwealth Scientific and Industrial Research Organisation, Hobart, TAS 7001, Australia.

H. Thomas, Department of Oceanography, University of Dalhousie, 1355 Oxford St., Halifax, NS B3H4 J1, Canada.

J.-L. Tison, Laboratoire de Glaciologie, DSTE, Université Libre de Bruxelles, Av. F. Roosevelt, CP 160/03, B-1050 Brussels, Belgium.